Research Journal of Applied Sciences, Engineering and Technology 4(20): 4066-4071, 2012
ISSN: 2040-7467

Submitted: March 10, 2012 Accepted: April 20, 2012 Published: October 15, 2012

Multifocus Image Fusion Combined Multiwavelet with Contourlet

[1]Yuelin Zou, [1]You Guo and [2]Liang Tian
[1]The Software Engineering Department, Shijiazhuang Information Engineering Vocational College, Shijiazhuang 050035, PR China
[2]College of Mathmatics and Information Science, Hebei Normal University, Shijiazhuang, PR China

Abstract: In this study, we propose a new image fusion method by combining Multiwavelet with Contourlet transform. Firstly, transform the source multifocus images successively by Multiwavelet and Conotourlet. Secondly, we employ the LEM rule to fuse the lowpass coefficients and PCCN rule to fuse the hightpass coefficients. Finally, inversely transform the fused coefficients successively by Contourlet and Multiwavelet. This algorithm is obviously better than Multiwavelet or Contourlet method in the fusion effect and the objective criterion of MI and $Q^{AB/F}$.

Keywords: Contourlet, LEM, multiwavelet, PCNN

INTRODUCTION

Because each kind of image sensor can only focus on a given different operating range and environmental conditions, it may not receive all the information necessary for detecting an object by human or computer vision (Pohl and van Genderen, 1998). Fused images may provide increased interpretation capabilities and more reliable results since data with different characteristics are combined (Wang, 2004).

Recently, image fusion methods based on multiscale decomposition, as a very important fusion method, has been widely used in image fusion area and has achieved great success. Multiwavelet, which is extension from scalar wavelets, have received considerable attention from the wavelets research communities both in theory as well as in applications such as signal compression and denoising (Gang and Min, 2000). Multiwavelets have several advantages in comparison with scalar wavelets on image processing, such features as short support, orthogonality, symmetry and vanishing moments, which are known to be important in image processing. An image fusion method based on Multiwavelet transform is proposed (Zhang *et al.*, 2005). The results of the experiment show that this image fusion based on Multiwavelet algorithm can get more satisfactory result. Do and Vetterli (2005) developed a true 2-D image representation method, namely, the Contourlet Transform (CT) (Duncan and Minh, 2006), which is achieved by combining the LP and the Directional Flter Bank (DFB). Compared with the traditional DWT, the CT is not only with multiscale and localization, but also with multidirectional and anisotropy. As a result, the CT can represent edges and other singularities along curves much more efficiently. However, the CT lacks the shift-invariance, which is desirable in many image applications such as image enhancement, image denoising and image fusion.

In this study, a new Multifocus Image Fusion algorithm is proposed based on combining the Multiwavelet transform with the Contourlet transform. After a multiscale decomposition of Multiwavelet, the Contourlet decomposition is used on the subimage of the Multiwavelet coefficient. The Local Energy Maximum (LEM) fusion rule is used in the low frequency subbands of the Contourlet coefficient. A new fusion method based on the PCNN is used for the high frequency subbands of the Contourlet coefficient. Finally, an inverse Contourlet and Multiwavelet is successively applied on the new fused coefficients to reconstruct the fused image.

METHODOLOGY

Multiwavelet: As in the scalar wavelet case, the theory of Multiwavelet is based on the idea of Multiresolution Analysis (MRA). The difference between them is that the Multiwavelet has two or more scaling and wavelet functions, but the wavelet has a single scaling function and a wavelet function. Its principle described in Shen *et al.* (2000).

The scaling functions of Multiwavelet are:

$$\Phi(t) = \left[\varphi_1(t), \varphi_2(t), \ldots, \varphi_r(t)\right]^T \quad (1)$$

Corresponding Author: Yuelin Zou, The software engineering department, Shijiazhuang Information Engineering Vocational College, Shijiazhuang 050035, PR China

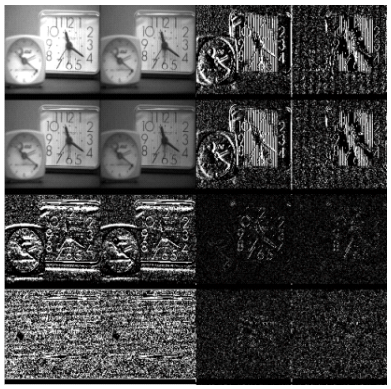

Fig. 1: Multiwavelet decomposition of the clock

The mother wavelet functions of Multiwavelet are defined as:

$$\varphi(t) = \left[\varphi_1(t), \varphi_2(t), \ldots, \varphi_r\ (t)\right]^T \qquad (2)$$

where, $\varphi_1(t)(1 = 1, 2, \ldots, r)$ are mutually orthogonal and $2^{j/2}\varphi_1(t)\ (2^j t\text{-}k)(j.k \in Z, 1 = 1, 2, \ldots, r)$ is an orthogonal basis of detailed subspaces on a certain scale space. *r* is generally set as 2 in the application of image processing (Xia *et al.*, 2010). The scaling functions and the wavelet functions of Multiwavelet satisfy the two-scale equation as following:

$$\begin{aligned} \Phi(t) &= \sqrt{2}\sum_{k=0}^{L} H_k \Phi(2t - k) \\ \Psi(t) &= \sqrt{2}\sum_{k=0}^{L} G_k \Psi(2t - k) \end{aligned} \qquad (3)$$

where, $0 \le k \le L$ and H_k and G_k are the *k*th $r \times r$ lowpass and highpass filter matrices, respectively. Multiwavelet consists of Geronimo, Hardin and Massopust (GHM), which contains two scaling functions and two Wavelet function. Multiwavelet transform decomposition is used on the two-dimensional image successively by row and by column. Multiwavelet decomposition of the clock image used to fuse experiments is shown in Fig. 1.

Contourlet: Contourlet was proposed by Do and Vetterli (2005). Contourlets were developed as an improvement over wavelets in terms of this inefficiency. The resulting transform has the multiscale and time-frequency-localization properties of wavelets, but also offers a high degree of directionality and anisotropy. It can efficiently represent contours and textures of an image. Contourlet is a double Filter Bank (FB) structure for obtaining sparse expansions for typical images with smooth contours, where, the LP is used to capture the point discontinuities firstly, then followed by a Directional Filter Bank (DFB) to link the point discontinuities into linear structures (Kun *et al.*, 2011). Figure 2a shows a multiscale and directional decomposition through the combination of LP and DFB. The overall result is an image expansion using basic elements like contour segments and thus named Contourlet. Figure 2b shows an example frequency partition of the Contourlet transform where the four scales are divided into 4, 4, 8 and 8 directional subbands from coarse to fine scales, respectively.

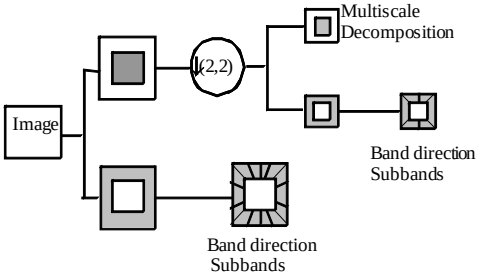

(a) decomposition framework

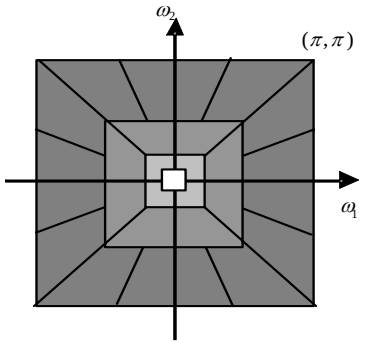

(b) frequency partition

Fig. 2: Contourlet transform

Proposed fusion algorithm: The flow diagram of the proposed algorithm is shown in Fig. 3 and implemented as:

Step 0: Perform GHM (Multiwavelet) decomposition on the source image A and image B and get the all coefficient including the LL, LH, HL and HH coefficients, G_A and G_B, defined in this study.

Step 1: Apply Contourlet transform on G_A and G_B (every subbands of the Multiwavelet decomposition). Decomposing the G_A and G_B by Contourlet transform. Get the Contourlet coefficients Cam, n (i, j) $C^B_{m,n}$(i, j) at a resolution scale *m* and

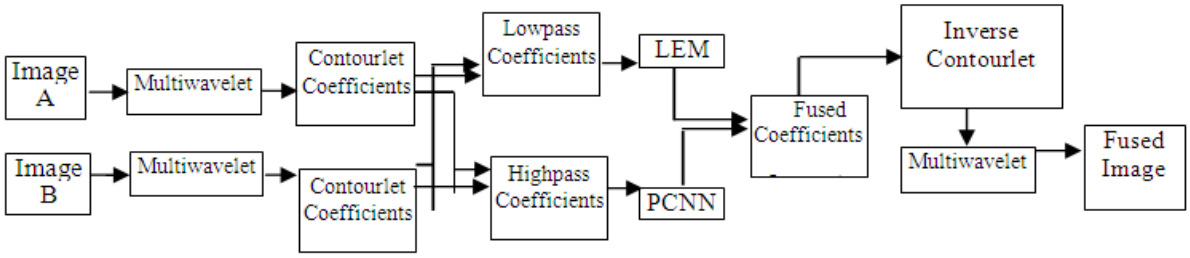

Fig. 3: Flow chart of proposed fusion algorithm

frequency direction *n*, from fine scales to coarse the number of the direction subbands of the DFB is 16, 8, 4 and 4, respectively. The decomposition level is set to 4.

Step 2: Perform the proposed fusion rules described in section of fusion rules to low frequency subbands and high-frequency direction subbands to generate the fused Contourlet coefficients $F_{m,n}(i, j)$.

Step 3: Reconstruct the G_F using fused coefficients $F_{m,n}(i, j)$ by inverse Contourlet transform.

Step 4: Perform inverse GHM (Multiwavelet) transform on the subimage G_F obtained above step to get the fused image F.

Fusion rules:

Fusion rule for low frequency coefficients: The Local Energy Maximum (LEM) fusion rule is effective and used to fuse the infrared and visible remote sensing images (Xia *et at*., 2010). In the low frequency subbands, the above rule is used in this study.

We first calculate the local energy features $E^A_{m,n}$ and $E^B_{m,n}$ of the low-frequency directional subbands of the two multifocus images. The local energy feature is defined as following:

$$Em,n(i.j) = \sqrt{\sum_{i\in p}\sum_{j\in q} W(i',j')\left[D_{m,n}(i+i',j+j')\right]^2} \quad (4)$$

where, $D_{m,n}(i+i', j+j')$ is the decomposition coefficients at the n^{th} direction subbands of the scale 2^{-m}. The local energy maximum can be calculate by convolving $D_{m,n}(i+i', j+j')$ with W. The size of the local window is $p\times q$ (p = 3 and q = 3). So, W is $\begin{bmatrix} 1/16 & 1/16 & 1/16 \\ 1/16 & 1/2 & 1/16 \\ 1/16 & 1/16 & 1/16 \end{bmatrix}$

So, the low frequency direction subband decision map is caculated by:

$$D^F_{m,n}(i,j) = \begin{Bmatrix} D^A_{m,n}(i.j), if \;\; E^A_{m,n}(i,j) \geq E^B_{m,n}(i,j) \\ D^B_{m,n}(i,j), \quad Other \end{Bmatrix} \quad (5)$$

Fusion rule for high frequency coefficients: PCNN is a feedback network and each PCNN neuron consists of three parts: the receptive field, modulation field and pulse generator (Ma *et al*., 2011). In PCNN model, the neuron receives input signals from feeding and linking inputs through the receptive field. The standard PCNN model is described as iteration by the following equations:

$$\begin{aligned} F_{ij}(t) &= \exp(-\alpha_F)F_{ij}(n-1) + V_F\sum_{ab} M_{ji,ab}Y_{ab}(t-1) + S_{ij} \\ L_{ij}(t) &= \exp(-\alpha_L)L_{ij}(t-1) + V_L\sum_{ab} M_{ij,ab}Y_{ab}(t-1) \\ U_{ij}(t) &= F_{ij}\left(1+\beta_j L_{ij}(t)\right) \\ Y_{ij}(t) &= \begin{cases} 1 & U_{ij}(n) > \theta_{ij}(t) \\ 0 & otherwise \end{cases} \\ \theta_{ij}(t) &= \exp(-\alpha_\theta)\theta_{ij}(t-1) + V_\theta Y_{ij}(t) \end{aligned} \quad (6)$$

In above formula, the *i* and *j* refer to the pixel location in the Contourlet high frequency coefficients. F_{ij} is feeding input and L_{ij} is linking input L_{ij}. S_{ij} is the input stimulus such as the gray level of image pixels in (*i, j*) position. U_{ij} is the internal activity of neuron and θ_{ij} is the dynamic threshold. Y_{ij} stands for the pulse output of neuron and it gets either the binary value 0 or 1. α_L, α_F and α_θ are the attenuation time constants of L_{ij}, F_{ij} and θ_{ij}, respectively. β_{ij} is the linking strength. V_F, V_L and V_θ denote the inherent voltage potential of F_{ij}, L_{ij} and θ_{ij}, respectively. *n* is the current iteration, where, *t* varies from 1 to $T_{max,}$ which is the total number of iterations and is set to 200 times. The model is elaborately described in study (Ma *et al*., 2011). The fusion rule is described as:

Take the high frequency subband $_{Cam,n}(i, j)$ and $_{Cbm,n}(i, j)$ separately as the feeding input to PCNN.

Let $L^k_{ij}(0) = U^k_{ij}(0) = 0$, $\theta^k_{ij}(0) = 1$, $L^k_{ij}(0) = U^k_{ij}(0) = 0$ and $Y^k_{ij}(0) = 0$in the *k*-th subband; i.e., each pixel does not fire.

Compute $L^k_{ij}(n)$,$U^k_{ij}(n)$, $Y^k_{ij}(n)$, $\theta^k_{ij}(n)$ according to Eq. (7)

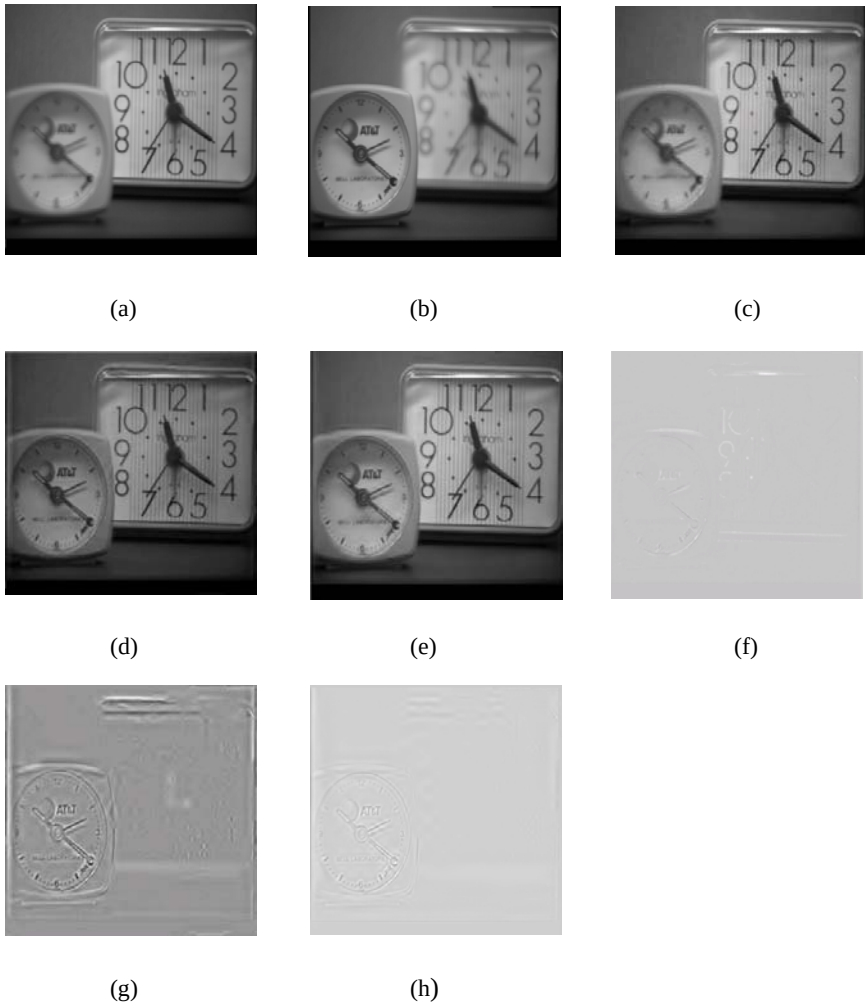

Fig. 4: The fusion results of 'Clock' image by different transform ((a) Image focus on the left; (b) Image focus on the right; (c)-(e) Fused image using multiwavelet, contourlet and proposed method; (f) Difference image between (c) and (a); (g) Difference image between (d) and (a); (h) Difference image between (e) and (a))

Firing times can be obtained by:

$$T_{i,j}^{l,k}(n) = T_{i,j}^{l,k}(n-1) + Y_{i,j}^{l,k}(n) \quad (7)$$

If $t = T_{max}$, then iteration stops. Then decision map $D^{l,k}_{i,j}$ can be calculated by (8)

$$D_{F,ij}^{l,k} = \begin{cases} 1, & if \quad T_{A,ij}^{l,k}(n) \geq T_{B,ij}^{l,k}(n) \\ 0, & if \quad T_{A,ij}^{l,k}(n) \leq T_{B,ij}^{l,k}(n) \end{cases} \quad (8)$$

Parameters of PCNN is set as p×q, $\alpha_L = 0.06931$, $\alpha_\theta = 0.2$, $\beta = 0.2$, $V_L = 1.0$, $V_\theta = 20$. $W = \begin{bmatrix} \sqrt{2} & 1 & \sqrt{2} \\ 1 & 0 & 1 \\ \sqrt{2} & 1 & \sqrt{2} \end{bmatrix}$

RESULTS AND DISCUSSION

Experiments: To evaluate the performance of the proposed fusion method, experiments with fusion one set of multifocus images 'Clock' and 'Pepsi' have been performed. The pair of the 'Clock' image and the pair of 'Pepsi' image fusion are shown in Fig. 4a, b and 5a, b.

For comparison purposes, in this study, the fusion is also performed using the Multiwavelet-based, the Contourlet-based method and proposed method, in all of which the subband coefficients are fusion by the proposed LME (lowpass subband) and PCNN (highpass subband) rule, respectively.

From Fig. 4c, h and 5c, h we can see that image fusing using proposed method can obtain a fusion image, on which the left part can be seen clearly than Multiwavelet and Contourlet method. The fusion result of

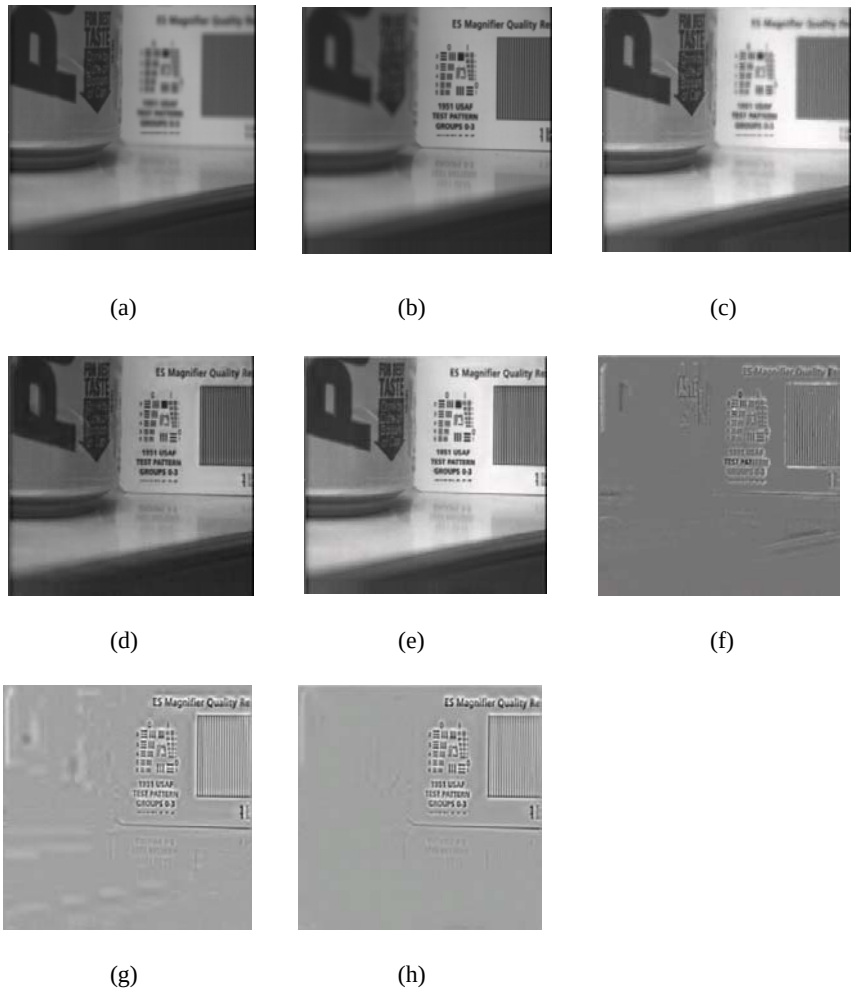

Fig. 5: The fusion results of 'Pepsi' image by different transform ((a)Image focus on the left; (b) Image focus on the right; (c)-(e) Fused image using multiwavelet, contourlet and proposed method; (f) Difference image between (c) and (a); (g) Difference image between (d) and (a); (h) Difference image between (e) and (a))

the Multiwavelet is most obscure in the left part of the image. The fusion result by Contourlet method is better than Multiwavelet method, but the proposed method is better than Contourlet method. I can be clealy seen from the difference with the source image A. It indicates that proposed method extracts the better characteristic than other two methods in multifocus images fusion.

For further comparison, two objective criteria are used to compare the fusion results. The first criterion is the Mutual Information (MI) metric proposed by Piella (2003). The second criterion is the $Q^{AB/F}$ metric, proposed by Xydeas and Petrovic (2000), which considers the amount of edge information transferred from the input images to the fused images. The values of MI and $Q^{AB/F}$ of fusion result of the multifocus image fusion are listed in the Table 1. All the objective criteria prove that the fused image of the proposed method is strongly correlated with the source images and more image features, i.e., edges, are preserved in the fusion process, suggesting that the proposed method does well in the multifocus image fusion outperforms the approach.

Table 1: The MI and $Q^{AB/F}$ by different transform

Images	Criteria	Multi-wavelet	CT	Proposed method
Clock	MI	5.8739	6.1840	6.3414
	$Q^{AB/F}$	0.5263	0.6392	0.6662
Pepsi	MI	5.9464	6.3645	6.5718
	$Q^{AB/F}$	0.5263	0.7176	0.7446

CONCLUSION

In this study, a method combing the Multiwavelet with Contourlet is proposed to fuse the multifocus images. The LME is used on the lowpass coefficients of the Contourlet transform and the PCNN is used to select the highpass Contourlet coefficients of the two source images. Some experiments are performed, comparing the new

algorithm with Contourlet and Multiwavelet fusion methods. The experimental results show that the proposed fusion rule is effective and the new algorithm can provide better performance in fusing image than Multiwavelet and Contourlet method.

REFERENCES

Do, M.N. and M. Vetterli, 2005. The contourlet transform: An efficient directional multiresolution image representation. IEEE T. Image Proc., 14(12): 2091-2106.

Duncan, D.Y.P. and N.D. Minh, 2006. Directional multiscale modeling of images using the contourlet transform. IEEE T. Image Proc., 15(6): 1610-1620.

Gang, L. and Z. Min, 2000. The application of multiwavelet transform to image coding. IEEE T. Image Proc., l9(2): 270-273.

Kun, L., G. Lei and C. Jingsong, 2011. Contourlet transform for image fusion using cycle spinning. J. Syst. Eng. Electron., 22(2): 353-357.

Ma, Y.,Y. Zhai, P. Geng and P. Yan, 2011. A novel algorithm of image fusion based on PCNN and Shearlet. Int. J. Digit. Content Technol. Appl., 5(12): 347-354.

Piella, G., 2003. A general framework for multiresolution image fusion: From pixels to regions. Inform. Fus., 4(4): 259-280.

Pohl, C. and J.L. van Genderen, 1998. Multisensor image fusion in remote sensing: Concepts methods and applications. Int. J. Rem. Sens., 19(5): 823-854.

Shen, L., H.H. Tan and J.Y. Tham, 2000. Symmetricantisym metric orthogonal multiwavelets and related scalar wavelet. Appl. Comput. Harmonic Anal., 8(3): 258- 279.

Wang, H.H., 2004. A new multiwavelet-based approach to image fusion. J. Math. Imag. Vis., 21(2): 177-192.

Xia, C., J. Licheng, L. Fang and X. Fangfang, 2010. Multi contourlet-based adaptive fusion of infrared and visible remote sensing images. IEEE Geosci. Rem. Sens. Lett., 7(3): 549-553.

Xydeas, C.S. and V. Petrovic, 2000. Objective image fusion performance measure. Electr. Lett., 36(4): 308-309.

Zhang, X.S., Q. Pan and Y.Q. Zhao, 2005. Image fusion method based on stationary multiwavelet transform. Guangdianzi Jiguang, 16(5): 605-609.